Monthly Notices
of the
ROYAL ASTRONOMICAL SOCIETY

Mon. Not. R. Astron. Soc. **420,** 2475–2479 (2012) doi:10.1111/j.1365-2966.2011.20211.x

Antitruncated stellar light profiles in the outer regions of STAGES spiral galaxies: bulge or disc related?

David T. Maltby,[1]★ Carlos Hoyos,[1] Meghan E. Gray,[1] Alfonso Aragón-Salamanca[1] and Christian Wolf[2]

[1]*School of Physics and Astronomy, The University of Nottingham, University Park, Nottingham NG7 2RD*
[2]*Department of Physics, Denys Wilkinson Building, University of Oxford, Keble Road, Oxford OX1 3RH*

Accepted 2011 November 16. Received 2011 November 15; in original form 2011 August 25

ABSTRACT

We present a comparison of azimuthally averaged radial surface brightness $\mu(r)$ profiles and analytical bulge–disc decompositions (de Vaucouleurs, $r^{1/4}$ bulge plus exponential disc) for spiral galaxies using *Hubble Space Telescope*/Advanced Camera for Surveys V-band imaging from the Space Telescope A901/2 Galaxy Evolution Survey (STAGES). In the established classification scheme, antitruncated $\mu(r)$ profiles (Type III) have a broken exponential disc with a shallower region beyond the break radius $r_{\rm brk}$. The excess light at large radii ($r > r_{\rm brk}$) can either be caused by an outer exponential disc (Type III-d) or an extended spheroidal component (Type III-s). Using our comparisons, we determine the contribution of bulge light at $r > r_{\rm brk}$ for a large sample of 78 (barred/unbarred, Sa-Sd) spiral galaxies with outer disc antitruncations ($\mu_{\rm brk} > 24\,{\rm mag\,arcsec^{-2}}$). In the majority of cases (∼85 per cent), evidence indicates that excess light at $r > r_{\rm brk}$ is related to an outer shallow disc (Type III-d). Here, the contribution of bulge light at $r > r_{\rm brk}$ is either negligible (∼70 per cent) or too little to explain the antitruncation (∼15 per cent). However in the latter cases, bulge light can affect the measured disc properties (e.g. $\mu_{\rm brk}$, outer scalelength). In the remaining cases (∼15 per cent), light at $r > r_{\rm brk}$ is dominated by the bulge (Type III-s). Here, for most cases the bulge profile dominates at all radii and only occasionally (three galaxies, ∼5 per cent) extends beyond that of a dominant disc and explains the excess light at $r > r_{\rm brk}$. We thus conclude that in the vast majority of cases antitruncated outer discs cannot be explained by bulge light and thus remain a pure disc phenomenon.

Key words: galaxies: spiral – galaxies: structure.

1 INTRODUCTION

The light profiles of spiral galaxies consist of two principal components: an inner, bulge-dominated component; and an outer exponentially declining disc with some minor deviations related to spiral arms (de Vaucouleurs 1959; Freeman 1970). However, since van der Kruit (1979) we have known that this 'classical' picture fails for most spiral galaxies, particularly at the faint surface brightness μ of the outer stellar disc. We now know that most disc profiles are best described by a two-slope model (broken exponential), characterized by an inner and outer exponential scalelength separated by a relatively well defined break radius $r_{\rm brk}$ (Pohlen et al. 2002). Many studies have now reported (mainly using surface photometry) the existence of broken exponential discs, or *truncations*, in spiral galaxies in both the local (Pohlen et al. 2002, 2007; Pohlen & Trujillo 2006; Bakos, Trujillo & Pohlen 2008; Erwin, Pohlen & Beckman 2008; Gutiérrez et al. 2011; Maltby et al. 2012) and distant $z < 1$ Universe (Pérez 2004; Trujillo & Pohlen 2005; Azzollini, Trujillo & Beckman 2008). Broken exponential discs have also been reported using resolved star counts on some nearby galaxies (Ibata et al. 2005; Ferguson et al. 2007).

These studies have resulted in a comprehensive classification scheme for disc galaxies based on break features in the outer disc component of their radial μ profiles (see e.g. Erwin, Beckman & Pohlen 2005; Pohlen & Trujillo 2006; Erwin et al. 2008). This scheme consists of three broad profile types (Type I, II and III): Type I (no break) – a single exponential disc extending out to several scalelengths (e.g. Bland-Hawthorn et al. 2005); Type II (down-bending break, *truncation*) – a broken exponential disc with a shallow inner and steeper outer region (van der Kruit 1979; Pohlen et al. 2002); Type III (up-bending break, *antitruncation*) – a broken exponential disc with a shallower region beyond the break radius $r_{\rm brk}$ (Erwin et al. 2005).

★E-mail: ppxdtm@nottingham.ac.uk

In the classical picture (simple bulge and disc), the de Vaucouleurs ($r^{1/4}$) bulge profile dominates in the centre while the exponential disc dominates at larger radii. However, theoretically the $r^{1/4}$ profile would dominate again at some low surface brightness. Erwin et al. (2005) suggest that in some Type III profiles (upbending breaks), the excess light beyond the break radius $r_{\rm brk}$ could be attributed to light from the spheroidal bulge or halo extending beyond the end of the disc. Consequently, Type III profiles can be separated into two distinct subclasses depending on whether the outer profile $r > r_{\rm brk}$ is dominated by a disc (Type III-d) or spheroidal component (Type III-s). Erwin et al. (2005) also propose that antitruncations with a smooth gradual transition and outer isophotes that are progressively rounder than that of the main disc, suggest an inclined disc embedded in a more spheroidal outer region such as an extended bulge or halo (i.e. Type III-s). Using this 'ellipse' method, previous works (Erwin et al. 2005, 2008; Gutiérrez et al. 2011) have found that ∼40 per cent of their Type III profiles are Type III-s.

However, the ellipse method is limited for face-on discs and cases where the outer/inner disc may have different orientations and axis ratios. In these instances, bulge–disc (B–D) decomposition (e.g. Allen et al. 2006) provides a useful tool to determine the contribution of the two major structural components (bulge and disc) to the galaxy's light distribution and should provide more conclusive evidence. The aim of this work is to use B–D decomposition on a large sample of 78 outer disc antitruncations from the Space Telescope A901/2 Galaxy Evolution Survey (STAGES; Gray et al. 2009) and assess the fraction of Type III profiles that show evidence for the excess light at large radii being caused or affected by the spheroidal component. This work builds on previous studies by using an improved method for the classification of Type III-s/III-d profiles (especially for face-on discs) and by using a larger more representative sample spanning the range of spiral morphologies.

Throughout this paper, we adopt a cosmology of $H_0 = 70\,{\rm km\,s^{-1}\,Mpc^{-1}}$, $\Omega_\Lambda = 0.7$ and $\Omega_{\rm m} = 0.3$, and use AB magnitudes unless stated otherwise.

2 DATA AND SAMPLE SELECTION

This work is entirely based on the STAGES data published by Gray et al. (2009). STAGES is an extensive multiwavelength survey targeting the Abell 901/2 multicluster system ($z \sim 0.167$) and covering a wide range of galaxy environments. *Hubble Space Telescope* (*HST*)/Advanced Camera for Surveys (ACS) *V*-band (*F606W*) imaging covering the full $0.^\circ5 \times 0.^\circ5$ ($\sim 5 \times 5\,{\rm Mpc}^2$) span of the multicluster system is complemented by extensive observations including photometric redshifts from Wolf et al. (2003). All imaging and data are publicly available.[1] In addition to this, all galaxies with apparent $R_{\rm vega} < 23.5$ mag and $z_{\rm phot} < 0.4$ (5090 galaxies) were visually classified by seven members of the STAGES team into the Hubble types (E, S0, Sa, Sb, Sc, Sd and Irr) and their intermediate classes (Gray et al., in preparation).

Our galaxy sample is drawn from Maltby et al. (2012). This consists of a large, mass-limited ($M_* > 10^9\,{\rm M}_\odot$), visually classified (Sa-Sdm, from Gray et al., in preparation) sample of 327 face-on to intermediate inclined ($i < 60^\circ$) spiral galaxies from both the field and cluster environments. However, we remove two galaxies for which B–D decomposition fails ($N_{\rm tot} = 325$). The 182 cluster spirals are at a redshift of $z_{\rm cl} = 0.167$ and the 143 field spirals span a redshift range of $0.05 < z_{\rm phot} < 0.30$. Maltby et al. (2012) analysed the $\mu(r)$ profiles for these galaxies in order to identify broken exponentials in the outer stellar disc $\mu > 24\,{\rm mag\,arcsec^{-2}}$ (their criteria for selecting intrinsically similar outer breaks). Three independent assessors agreed on a subsample of 78 antitruncated (Type III) outer μ profiles ($\mu_{\rm brk} > 24\,{\rm mag\,arcsec^{-2}}$). We shall use both this Type III subsample and the total sample in this work.

[1] http://www.nottingham.ac.uk/astronomy/stages

3 METHODOLOGY

For each galaxy in our sample, we perform a two-dimensional B–D decomposition based on a two-component galaxy model comprising a de Vaucouleurs ($r^{1/4}$) bulge and a single exponential disc. Decompositions were carried out on the STAGES *V*-band imaging using the GALFIT code (Peng et al. 2002) and the method of Hoyos et al. (2012) adapted to perform two-component fits. Several measurable properties are produced for each galaxy including position [*x*,*y*], effective radii, total magnitudes, axis ratios, position angles for the bulge and disc components and a sky-level estimation.

B–D decomposition can be sensitive to the initial conditions used to search the B–D parameter space (e.g. initial guess for bulge-to-disc ratio *B*/*D*). Therefore, we perform two runs of the B–D decomposition with different initial conditions from the two extremes: one run starting from a bulge-dominated system ($B/D = 9$) and the other run starting from a disc-dominated system ($B/D = 1/9$). Comparison of these runs (hereafter Run 1 and Run 2) allows for an assessment of the uniqueness/stability of B–D decomposition on a galaxy–galaxy basis. In the vast majority of cases (∼85 per cent) the results were effectively the same, ∼70 per cent being exactly the same and ∼15 per cent having only minor differences that do not affect our analysis (*B*/*D* the same within ∼10 per cent). In a few cases (∼10 per cent), the decomposition was catastrophically unstable with Run 1/2 yielding both bulge- and disc-dominated systems. The remaining cases (∼5 per cent) showed moderate instabilities great enough to affect the assessment of bulge light in the outer regions of the galaxy. These stability fractions are the same in our Type III subsample. The unstable solutions are mainly driven by differences in the sky level determined during the decomposition. However, the overall conclusions of this work are not affected by these unstable solutions.

For each galaxy, we also use the IRAF task ellipse (STSDAS package – version 2.12.2) in order to obtain azimuthally averaged radial $\mu(r)$ profiles from the STAGES *V*-band imaging, see Maltby et al. (2012) for full details of the ellipse fitting method used. For all our ellipse fits the galaxy centre is fixed (all isophotes have a common centre) using the galaxy centre determined during B–D decomposition. The bad pixel masks of Gray et al. (2009) are also used to remove everything not associated with the galaxy itself from the isophotal fit (e.g. light from companion galaxies).

Using a procedure similar to previous works (Pohlen & Trujillo 2006; Erwin et al. 2008), we fit two different sets of ellipses to each galaxy image. The first is a free-parameter fit (fixed centre, free ellipticity *e* and position angle PA) and tends to follow morphological features such as bars and spiral arms. Consequently, these free-parameter fits are not suitable for the characterization of the underlying outer disc; however, they may be used to determine the *e* and PA of the outer disc component, see Maltby et al. (2012) for further details. A fixed-parameter fit (fixed centre, *e* and PA using the *e* and PA determined for the outer disc) is then used to produce our final measured $\mu(r)$ profiles. The necessary sky subtraction is then performed using the sky-level estimates generated during B–D

decomposition. Please note that these sky values sometimes differ slightly from those of Maltby et al. (2012).

Analogous fixed-parameter fits (using the e and PA determined for the outer disc) are also carried out on the disc-residual images (ACS image – bulge-only model) resulting in a measured μ profile for the disc component $\mu_{\rm Disc}(r)$. We also obtain azimuthally averaged radial μ profiles for the decomposed B–D model using the same fixed-parameter ellipses (isophotes) as in the other profiles. These yield separate radial μ profiles for both the disc and bulge model along the semimajor axis of the outer disc.

All resultant μ profiles are corrected for Galactic foreground extinction, individual galaxy inclination i and surface brightness dimming (the μ profiles of field galaxies, $0.05 < z_{\rm phot} < 0.30$, are corrected to the redshift of the cluster $z = 0.167$). Full details of the fitting procedure, subsequent photometric calibration and an estimation of the error in the sky subtraction (± 0.18 counts) can be found in Maltby et al. (2012).

4 RESULTS

B–D decompositions using a de Vaucouleurs ($r^{1/4}$) bulge plus an exponential disc can be classified into four distinct profile types (e.g. Allen et al. 2006), see Fig. 1.

(1) *Type A*: 'classical' system. The bulge profile dominates at the centre, while the disc profile dominates at large radii. The bulge/disc profiles cross only once.

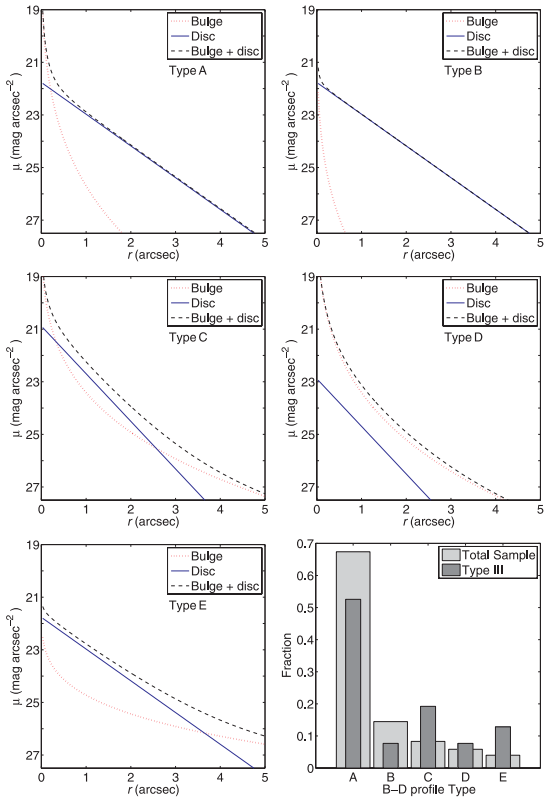

Figure 1. Bulge–disc profile types. Top left: Type A, 'classical' profile. Top right: Type B, disc-dominated profile. Middle left: Type C, bulge dominated at small/large radii but disc dominated at intermediate radii. Middle right: Type D, bulge dominated. Bottom left: Type E, 'constrained' outer bulge. Bottom right: profile type distributions for the total sample and Type III subsample.

(2) *Type B*: disc-dominated system. The disc profile dominates at all radii, with a weak contribution from the bulge in the centre. The bulge/disc profiles never cross.

(3) *Type C*: the bulge profile dominates at small/large radii, but the disc profile dominates at intermediate radii.

(4) *Type D*: bulge-dominated system. The bulge profile dominates at all radii with a weak underlying disc component. The bulge/disc profiles never cross.[2]

In addition to this, we also observe decompositions where the disc profile dominates in the centre, while the bulge profile dominates at large radii (hereafter Type E). Here, we believe that an outer antitruncated disc has incorrectly affected the bulge profile fit. In these cases, B–D decomposition is not a true representation of the galaxy at large radii and these galaxies probably have Type B like compositions. Similar constraints may also occur in some Type D profiles.

Fig. 1 shows the distribution of B–D profile types for both the total sample and the Type III subsample. As expected, the fraction of Type C/E profiles is greater in the Type III subsample. For the total sample, several other correlations between B–D profile type, Hubble-type morphology (Sa-Sd) and measured B/D ratio are observed. Type A/B profiles are equally probable in all Hubble types but Type C/D profiles are more common in earlier Hubble types (Sa-Sb). Also as expected, mean/median B/D decreases with progressively later Hubble types and increases for the sequence of B–D profile types B–A–C–D (increasing bulge dominance).

For each galaxy in our Type III subsample, we compared the measured, fixed ellipse $\mu(r)$ profile with the model μ profiles from the B–D model in order to assess the contribution of bulge light in the outer regions of the galaxy ($r > r_{\rm brk}$). Fig. 2 shows some examples for each B–D profile type. These comparisons resulted in three possible scenarios. Bulge light in the outer profile ($r > r_{\rm brk}$) had:

(i) *little or no contribution* (∼70 per cent): for all Type A/B profiles the bulge contributes virtually no light at $r > r_{\rm brk}$ and in some Type C/E profiles the contribution is negligible. This can be determined by inspection of the measured disc-residual profile $\mu_{\rm Disc}(r)$ and assessing if the properties of the outer profile/break ($r_{\rm brk}$, $\mu_{\rm brk}$, scalelength) have been affected with respect to the sky-subtraction error. No Type D profiles are in this category.

(ii) *minor contribution* (∼15 per cent): approximately half of these cases are Type C profiles where the bulge profile emerges from the end of the disc and contributes some light to the outer regions of the galaxy. The remaining half are Type E profiles where the bulge appears to be constrained by an outer exponential disc. The amount contributed is enough to affect the outer profile causing $\mu_{\rm brk}$ and the outer scalelength to be different in the disc-residual profile $\mu_{\rm Disc}(r)$. However, the antitruncation remains present.

(iii) *major contribution* (∼15 per cent): here, the bulge contributes the majority of the light at $r > r_{\rm brk}$. Approximately half of these cases are Type D profiles where the bulge dominates at all radii. For these cases, the de Vaucouleurs profile is either interpreted as an antitruncation or being constrained by an outer shallow disc. The remaining half are all Type C profiles (with one exception which is Type E). In these latter cases the antitruncation is not observed in the disc-residual profile $\mu_{\rm Disc}(r)$, see Fig. 3 for such an example.

[2] Note the use of capital letters in profile types to avoid confusion with other classification schemes.

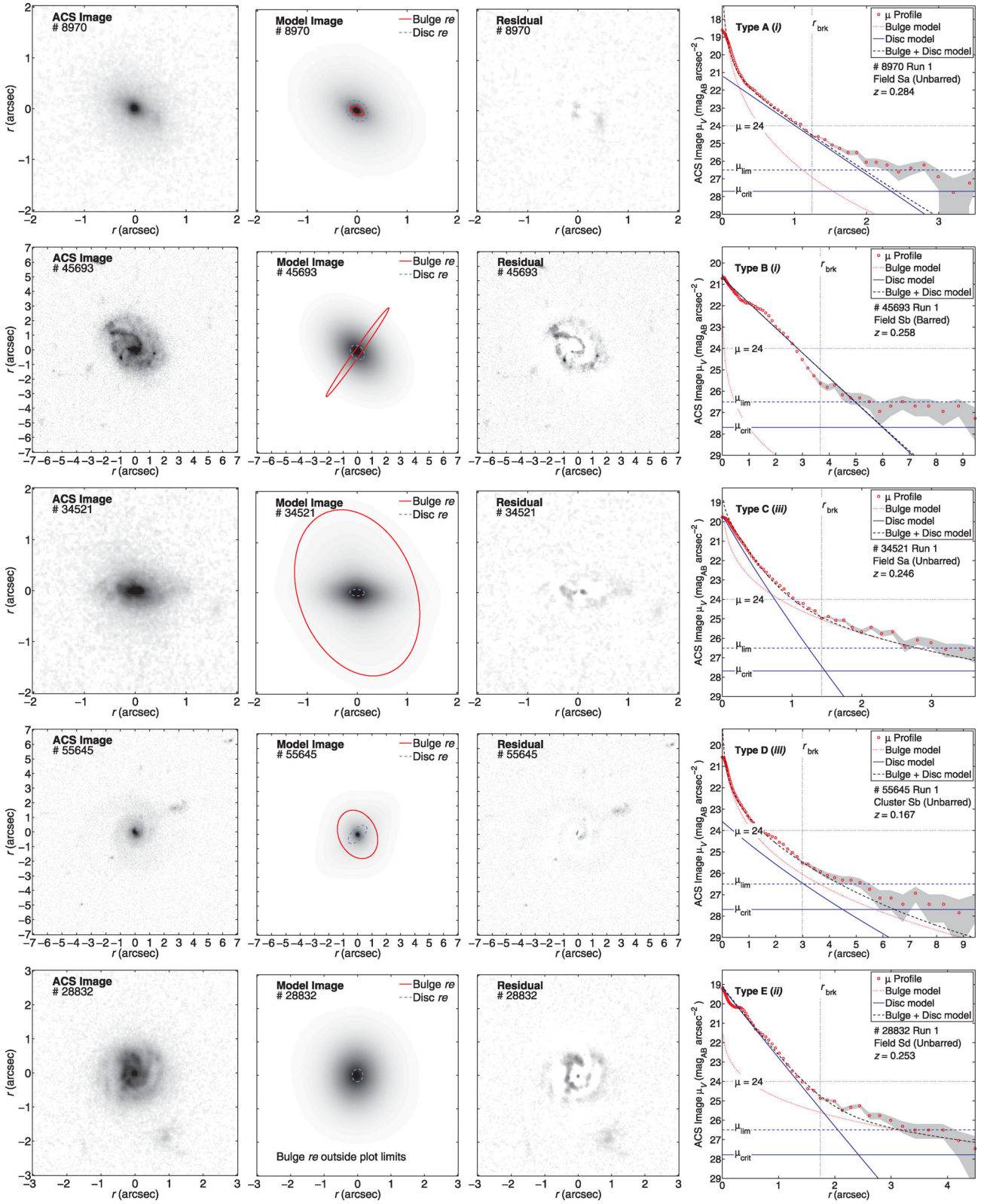

Figure 2. Example B–D decompositions and antitruncated μ profiles. Rows, top to bottom: decompositions producing Type A, Type B, Type C, Type D and Type E profiles. The bulge (red dotted line), disc (blue line) and bulge + disc (black dashed line) profiles from B–D decomposition are overplotted on the measured μ profiles (red circles). The i/ii/iii notation after the profile type indicates whether the bulge profile has a negligible, minor or major contribution outside the break radius $r > r_{\rm brk}$, as explained in Section 4. Errors in the measured μ profiles are for an oversubtraction and an undersubtraction of the sky by $\pm 1\sigma$. The $\mu_{\rm crit}/\mu_{\rm lim}$ levels represent $+1\sigma/+3\sigma$ above the sky, respectively, see Maltby et al. (2012) for full details. The model images show the effective radius isophote for both the bulge (red line) and disc (blue dashed line) models.

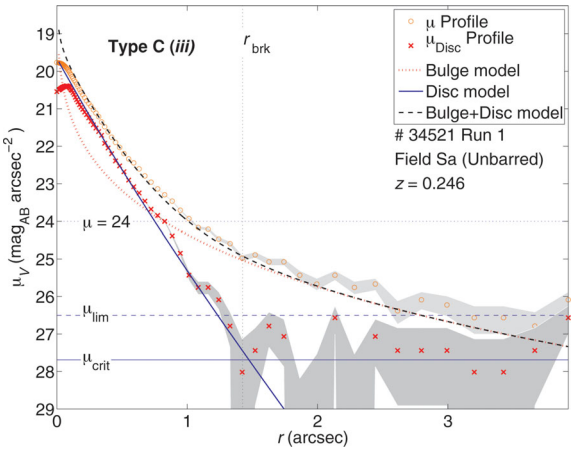

Figure 3. A rare/unusual example of a bulge profile causing an antitruncation in a μ profile (Type C example from Fig. 2, break radius r_{brk}). The bulge (red dotted line), disc (blue line) and bulge + disc (black dashed line) profiles from B–D decomposition are overplotted on the measured μ profile (red circles). The disc-residual μ_{Disc} profile (measured μ profile minus bulge-only model, red crosses) shows no antitruncation (for errors, see Fig. 2).

5 CONCLUSIONS

Our results suggest that for the majority of Type III profiles (∼85 per cent), the excess light beyond the break radius r_{brk} is related to an outer shallow disc (Type III-d). However, it is important to note that for some of these cases (∼15 per cent), bulge light can affect the properties of the disc profile (e.g. μ_{brk}, outer scalelength). For the remaining Type III profiles (∼15 per cent), the excess light at $r > r_{brk}$ can be attributed to the bulge profile (Type III-s). However, few of these latter cases (only three galaxies with stable decompositions, ∼5 per cent) exhibit profiles where the bulge profile extends beyond a dominant disc (Type C) and causes an antitruncation in the μ profile.

Previous works (Erwin et al. 2008; Gutiérrez et al. 2011) have used the ellipse method to classify their Type III-d/III-s profiles. The results of these works are in good agreement with their Type III profiles being ∼60 per cent Type III-d and ∼40 per cent Type III-s. These results appear *not* to be consistent with our results. However, consider the case where the contribution of bulge light at $r > r_{brk}$ is too little to explain the antitruncation but great enough to affect the properties of the profile. The increased contribution of bulge light to the $\mu(r)$ profile at r_{brk} could lead to a smoothing of the inflection and a roundening of the outer isophotes. Therefore, using the ellipse method would likely have resulted in these Type III-d profiles being classified as Type III-s. Applying this reasoning to our results, we obtain fractions of ∼70/30 per cent for Type III-d/III-s profiles, respectively. Therefore, the ellipse method potentially could lead to genuine disc breaks being classified as Type III-s. Our method offers an improved way to determine whether an antitruncation is disc or spheroid related.

However, our method does have some obvious drawbacks. In a two-component B–D decomposition, an outer antitruncated disc could cause the bulge profile to be constrained and lead to an overestimation of bulge light in the outer regions of the galaxy. This naturally enhances our fraction of Type III-s profiles which therefore represents an upper limit to the fraction of genuine Type III-s profiles in our Type III sample. Therefore, we can conclude that in the vast majority of cases Type III profiles are indeed a true disc phenomenon.

Several studies have proposed formation scenarios for Type III profiles, mainly via satellite accretion or minor mergers (Peñarrubia, McConnachie & Babul 2006; Younger et al. 2007). A discussion of these scenarios is beyond the scope of this work. However, we do make one important comment. Previous works (e.g. Pohlen & Trujillo 2006; Maltby et al. 2012) have reported that Type III profiles are more frequent in earlier Hubble types. This result is consistent with a minor merger scenario for their origin. However, the excess Type III profiles in early types could easily have been related to a natural increase in the number of Type III-s profiles in earlier Hubble types. Fortunately, we observe exactly the same relations using just our genuine Type III-d profiles and thus our results remain consistent with the minor merger scenario for the formation of Type III profiles.

ACKNOWLEDGMENTS

We wish to thank the anonymous referee for their very careful reading and detailed comments on the original version of this paper which have helped us to vastly improve it. We also thank Stephen Bamford for useful discussions. The support for STAGES was provided by NASA through GO-10395 from STScI operated by AURA under NAS5-26555. DTM and MEG were supported by STFC. CH acknowledges support from a Spanish MEC post-doctoral fellowship.

REFERENCES

Allen P. D., Driver S. P., Graham A. W., Cameron E., Liske J., de Propris R., 2006, MNRAS, 371, 2
Azzollini R., Trujillo I., Beckman J. E., 2008, ApJ, 684, 1026
Bakos J., Trujillo I., Pohlen M., 2008, ApJ, 683, L103
Bland-Hawthorn J., Vlajić M., Freeman K. C., Draine B. T., 2005, ApJ, 629, 239
de Vaucouleurs G., 1959, Handbuch Phys., 53, 311
Erwin P., Beckman J. E., Pohlen M., 2005, ApJ, 626, L81
Erwin P., Pohlen M., Beckman J. E., 2008, AJ, 135, 20
Ferguson A., Irwin M., Chapman S., Ibata R., Lewis G., Tanvir N., 2007, in de Jong R. S., ed., Resolving the Stellar Outskirts of M31 and M33. Springer, Dordrecht, p. 239
Freeman K. C., 1970, ApJ, 160, 811
Gray M. E. et al., 2009, MNRAS, 393, 1275
Gutiérrez L., Erwin P., Aladro R., Beckman J. E., 2011, AJ, 142, 145
Hoyos C. et al., 2012, MNRAS, 419, 2703
Ibata R., Chapman S., Ferguson A. M. N., Lewis G., Irwin M., Tanvir N., 2005, ApJ, 634, 287
Maltby D. T. et al., 2012, MNRAS, 419, 669
Peñarrubia J., McConnachie A., Babul A., 2006, ApJ, 650, L33
Peng C. Y., Ho L. C., Impey C. D., Rix H.-W., 2002, AJ, 124, 266
Pérez I., 2004, A&A, 427, L17
Pohlen M., Trujillo I., 2006, A&A, 454, 759
Pohlen M., Dettmar R., Lütticke R., Aronica G., 2002, A&A, 392, 807
Pohlen M., Zaroubi S., Peletier R. F., Dettmar R., 2007, MNRAS, 378, 594
Trujillo I., Pohlen M., 2005, ApJ, 630, L17
van der Kruit P. C., 1979, A&AS, 38, 15
Wolf C., Meisenheimer K., Rix H.-W., Borch A., Dye S., Kleinheinrich M., 2003, A&A, 401, 73
Younger J. D., Cox T. J., Seth A. C., Hernquist L., 2007, ApJ, 670, 269

This paper has been typeset from a TEX/LATEX file prepared by the author.